

Quantum Chemical Investigations and Bonding Analysis of Iron Complexes with Mixed Cyano and Carbonyl Ligands†

Christoph Loschen and Gernot Frenking*

Fachbereich Chemie der Philipps-Universität Marburg, Hans-Meerwein-Strasse, D-35043 Marburg, Germany

Received July 11, 2003

The equilibrium structures and vibrational frequencies of the iron complexes $[\text{Fe}(\text{CN})_x(\text{CO})_y]^q$ ($x = 0-6$ and $y = 0-5$) have been calculated at the BP86 level of theory. The nature of the Fe–CN and Fe–CO has been analyzed with an energy partitioning method. The calculated Fe–CO bond lengths are in good agreement with the results of X-ray structure analysis whereas the Fe–CN bonds are calculated somewhat longer than the experimental values. The theoretically predicted vibrational frequencies of the C–O stretching mode are always lower and the calculated CN[−] frequencies are higher than the observed fundamental modes. The results of the bonding analysis suggest that the Fe–CO binding interactions have ~55% electrostatic character and ~45% covalent character. There is a significant contribution of the π orbital interaction to the Fe–CO covalent bonding which increases when the complexes become negatively charged. The strength of ΔE_π may even be larger than ΔE_σ . The Fe–CN[−] bonds have much less π character. The calculated binding energy of the Fe–CO π -interactions correlates very well with the C–O stretching frequencies.

Introduction

Iron complexes with CO and CN[−] ligands have become the focus of intensive experimental investigations in recent years¹ because Fe(CN)(CO) moieties were found to be catalytic centers in hydrogenase enzymes.² From a physiological point of view, it is remarkable to find carbonyl and cyano groups as native ligands in metallo proteins. In order to understand the reactivities of the latter species, it would be helpful to know about the structures and properties of mixed iron carbonyl cyano complexes $[\text{Fe}(\text{CN})_n(\text{CO})_{6-n}]^q$, but only some members of this family of Fe(II) complexes are known. Recently, Koch and co-workers succeeded in the

synthesis of the complexes *trans*- $[\text{Fe}(\text{CN})_4(\text{CO})_2]^{2-}$,³ *cis*- $[\text{Fe}(\text{CN})_4(\text{CO})_2]^{2-}$, and *fac*- $[\text{Fe}(\text{CN})_3(\text{CO})_3]^{1-}$.⁴ Together with the compounds $[\text{Fe}(\text{CN})_6]^{4-}$,^{5,6} $[\text{Fe}(\text{CN})_5\text{CO}]^{3-}$,^{7,8} and $[\text{Fe}(\text{CN})(\text{CO})_4]^{1-}$ ⁹ synthesized in the 18th, 19th, and 20th centuries, respectively, one obtains a series of similar compounds which is well suited for a comparative theoretical investigation. In order to analyze the bonding situation in the hexacoordinated iron complexes with cyano and carbonyl ligands and to

* To whom correspondence should be addressed. E-mail: frenking@chemie.uni-marburg.de.

† Theoretical Studies of Inorganic Compounds. 26. Part 25: Lein, M.; Frunzke, J.; Frenking, G. *Inorg. Chem.* **2003**, *42*, 2504.

(1) (a) Hsu, H.-F.; Koch, S. A.; Popescu, C. V.; Münck, E. *J. Am. Chem. Soc.* **1997**, *119*, 8371. (b) Lai, C. H.; Lee, W. Z.; Miller, M. L.; Reibenspies, J. H.; Darenbourg, D. J.; Darenbourg, M. Y. *J. Am. Chem. Soc.* **1998**, *120*, 10103. (c) Liaw, W. F.; Lee, N. H.; Chen, C. H.; Lee, C. M.; Lee, G. H.; Peng, S. M. *J. Am. Chem. Soc.* **2000**, *122*, 488. (d) Darenbourg, M. Y.; Lyon, E. J.; Smees, J. J. *Coord. Chem. Rev.* **2000**, *206*, 533. (e) Schmidt, M.; Contakes, S. M.; Rauchfuss, T. B. *J. Am. Chem. Soc.* **1999**, *121*, 9736. (f) Lyon, E. J.; Georgakaki, I. P.; Reibenspies, J. H.; Darenbourg, M. Y. *Angew. Chem.* **1999**, *111*, 3373; *Angew. Chem., Int. Ed.* **1999**, *38*, 3178. (g) Cloirec, A. L.; Best, S. P.; Borg, S.; Davies, S. C.; Evans, D. J.; Hughes, D. L.; Pickett, C. J. *Chem. Commun.* **1999**, 2285.

(2) (a) Fontecilla-Camps, J. C.; Ragsdale, S. W. *Adv. Inorg. Chem.* **1999**, *47*, 283. (b) Adams, M. W. W.; Stiefel, E. I. *Curr. Opin. Chem. Biol.* **2000**, *4*, 214. (c) Peters, J. W. *Curr. Opin. Struct. Chem. Biol.* **1999**, *9*, 670. (d) Pierik, A. J.; Rosenboom, W.; Happe, R. P.; Bagley, K. A.; Albracht, S. P. J. *J. Biol. Chem.* **1999**, *274* (6), 3331. (e) Volbeda, A.; Garcia, E.; Piras, C.; Delacey, A. L.; Fernandez, V. M.; Hatchikian, E. C.; Frey, M.; Fontecilla-Camps, J. C. *J. Am. Chem. Soc.* **1996**, *118*, 12989. (f) Peters, J. W.; Lanzilotta, W. N.; Lemon, B. J.; Seefeldt, L. C. *Science* **1998**, *282*, 1853. (g) Nicolet, Y.; Piras, C.; Legrand, P.; Hatchikian, C. E.; Fontecilla-Camps, J. C. *Structure (London)* **1999**, *7*, 13.

(3) Jiang, J.; Koch, S. A. *Angew. Chem., Int. Ed.* **2001**, *28*, 992.

(4) Jiang, J.; Koch, S. A. *Inorg. Chem.* **2002**, *41* (2), 158.

(5) *Miscellanea Berolinensia ad incrementum scientiarum*; Berlin, 1710; p 377.

(6) Buser, H. J.; Schwarzenbach, D.; Petter, W.; Ludi, A. *Inorg. Chem.* **1977**, *16*, 2704.

(7) Muller, J. A. C. R. *Hebd. Seances Acad. Sci.* **1887**, *104*, 992.

(8) Jiang, J.; Acunzo, A.; Koch, S. A. *J. Am. Chem. Soc.* **2001**, *123*, 12109.

(9) (a) Goldfield, S. A.; Raymond, K. N. *Inorg. Chem.* **1974**, *13*, 770. (b) Jones, L. H.; McDowell, R. S.; Goldblatt, M.; Swanson, B. I. *J. Chem. Phys.* **1972**, *57*, 2050. (c) Braga, D.; Grepioni, F.; Orpen, A. G. *Organometallics* **1993**, *12*, 1481.

predict theoretically the structures and properties of the yet unknown molecules *mer*-[Fe(CN)₃(CO)₃]¹⁻, *trans*-[Fe(CN)₂(CO)₄], *cis*-[Fe(CN)₂(CO)₄], and [FeCN(CO)₅]¹⁺, we carried out quantum chemical calculations using DFT methods of the geometries, bond energies, and vibrational frequencies of the isoelectronic compounds [Fe(CN)_n(CO)_{6-n}]^q. We additionally calculated the pentacoordinated complexes [FeCN(CO)₄]¹⁻ and [Fe(CO)₅] and the Fe(III) complex [Fe(CN)₅CO]²⁻.

The interactions of a transition metal with the isoelectronic ligands CO and CN⁻ are usually discussed in terms of the donor–acceptor model of Dewar, Chatt, and Duncanson^{10,11} (DCD). Experimental findings suggest that π -back-donation is very important for most carbonyl complexes¹² while cyano ligands bind mainly through σ -donation.¹³ We investigated the iron–carbonyl and iron–cyano interactions with an energy partitioning analysis (EPA)^{14,15} that has been found very useful for investigating the nature of the bonding in donor–acceptor complexes.¹⁶ The advantage of the EPA method is that it gives not only a quantitative estimate of the energy contributions of the σ -donation and π -back-donation but also a quantitative estimate of the electrostatic contributions and the Pauli repulsion to the chemical bonding.

IR spectroscopy is a very important analytical tool to experimentally investigate this kind of transition metal complex. Therefore, for the experimentally yet unknown compounds the prediction of their vibrational spectra (Raman and IR) should be useful in order to identify them spectroscopically. For the experimentally known complexes, we report in this paper about a comparison of calculated C–O and C–N⁻ vibrational frequencies with the corresponding experimental values. Thorough studies of C–O vibrational modes of pure transition metal carbonyl complexes have been performed by Thiel and Frenking.^{17–19} They could show that the BP86 functional performs best among the available DFT functionals to predict vibrational data for this class of compounds. The topic of this paper is a theoretical study of the structures, vibrational spectra, and bonding analysis of the complexes [Fe(CN)₆]⁴⁻ (**1**), [Fe(CN)₅CO]³⁻ (**2**), *trans*-[Fe(CN)₄(CO)₂]²⁻ (**3-trans**), *cis*-[Fe(CN)₄(CO)₂]²⁻ (**3-cis**), *fac*-[Fe(CN)₃(CO)₃]¹⁻ (**4-fac**), *mer*-[Fe(CN)₃(CO)₃]¹⁻ (**4-mer**), *trans*-[Fe(CN)₂(CO)₄] (**5-trans**), *cis*-[Fe(CN)₂(CO)₄] (**5-cis**), [FeCN(CO)₅]¹⁺ (**6**), [FeCN(CO)₄]¹⁻ (**7**), [Fe(CO)₅] (**8**), and [Fe(CN)₅CO]²⁻ (**9**).

(10) Dewar, M. J. S. *Bull. Soc. Chim. Fr.* **1951**, 18, C79.

(11) Chatt, J.; Duncanson, L. A. *J. Chem. Soc.* **1953**, 2929.

(12) (a) Elschenbroich, Ch.; Salzer, A. *Organometallics*, 2nd ed.; VCH: Weinheim, 1992. (b) Transition metal carbonyl complexes with little π back-donation (nonclassical carbonyl complexes) may also be quite stable: Lupinetti, A. J.; Strauss, S. H.; Frenking, G. *Progress in Inorganic Chemistry*; Karlin, K. D., Ed.; Wiley: New York, 2001; Vol. 49, p 1.

(13) (a) Ehlers, A. W.; Dapprich, S.; Vyboishchikov, S. F.; Frenking, G. *Organometallics* **1996**, 15, 105. (b) Dietz, O.; Rayón, V. M.; Frenking, G. *Inorg. Chem.* **2003**, 42, 4977.

(14) Morokuma, K. *J. Chem. Phys.* **1971**, 55, 1236.

(15) Ziegler, T.; Rauk, A. *Theor. Chim. Acta* **1977**, 46, 1.

(16) Frenking, G.; Wichmann, K.; Fröhlich, N.; Loschen, C.; Lein, M.; Frunzke, J.; Rayón, V. M. *Coord. Chem. Rev.* **2003**, 238–239, 55.

(17) Jonas, V.; Thiel, W. *J. Chem. Phys.* **1995**, 102, 8474.

(18) Jonas, V.; Thiel, W. *Organometallics* **1998**, 17, 353.

(19) Szilagy, R. K.; Frenking, G. *Organometallics* **1997**, 16, 4807.

Theoretical Methods

The geometries of the molecules have been optimized at the nonlocal DFT level of theory using the exchange functional of Becke²⁰ and the correlation functional of Perdew²¹ (BP86). The calculations of the energy minimum structures and the vibrational frequencies have been carried out with the program package Gaussian 98,²² which allows analytical calculations of the second derivatives of the BP86 energy functionals with respect to the nuclear coordinates. The calculation of the bonding energy and the EPA were carried out using ADF.²³

For the frequency calculations we used a 6-31G(d) basis set for carbon, nitrogen, and oxygen and a nonrelativistic small-core ECP for iron with a (441/2111/41) valence basis set derived from the (55/5/5) basis of Hay and Wadt.²⁴ This basis set combination has been introduced as standard basis set II.²⁵ All optimized structures were found to be energy minima at BP86/II.

The EPA calculations with ADF were carried out at the BP86 level using uncontracted Slater orbitals (STOs)²⁶ with triple- ζ quality in the valence region and double- ζ quality in the core region augmented by one set of polarization function (TZP) using geometries that were optimized at BP86/TZP. Relativistic effects were accounted for by the zero order regular approximation (ZORA).²⁷ The (1s)² core electrons of carbon, oxygen, and nitrogen and the (1s2s2p)¹⁰ core electrons of iron were treated by the frozen core approximation.²⁸

The EPA method of ADF is based upon the energy decomposition analysis developed independently by Morokuma¹⁴ and by Ziegler and Rauk.¹⁵ In this method the instantaneous interaction energy (ΔE_{int}) between the two fragments can be divided into three components

$$\Delta E_{\text{int}} = \Delta E_{\text{elstat}} + \Delta E_{\text{Pauli}} + \Delta E_{\text{orb}} \quad (1)$$

where ΔE_{elstat} gives the electrostatic interaction energy between the fragments, which have been calculated with a frozen electron density distribution in the geometry of the complex. ΔE_{Pauli} gives the repulsive four-electron interactions between occupied orbitals, and ΔE_{orb} gives the stabilizing orbital interactions. Since ΔE_{orb} can be considered as an estimate of the covalent contributions to the

(20) Becke, A. D. *Phys. Rev. A* **1988**, 38, 3098.

(21) Perdew, J. P. *Phys. Rev. B* **1986**, 33, 8822.

(22) Frisch, M. J.; Trucks, G. W.; Schlegel, H. B.; Scuseria, G. E.; Robb, M. A.; Cheeseman, J. R.; Zakrzewski, V. G.; Montgomery, J. A., Jr.; Stratmann, R. E.; Burant, J. C.; Dapprich, S.; Millam, J. M.; Daniels, A. D.; Kudin, K. N.; Strain, M. C.; Farkas, O.; Tomasi, J.; Barone, V.; Cossi, M.; Cammi, R.; Mennucci, B.; Pomelli, C.; Adamo, C.; Clifford, S.; Ochterski, J.; Petersson, G. A.; Ayala, P. Y.; Cui, Q.; Morokuma, K.; Malick, D. K.; Rabuck, A. D.; Raghavachari, K.; Foresman, J. B.; Cioslowski, J.; Ortiz, J. V.; Stefanov, B. B.; Liu, G.; Liashenko, A.; Piskorz, P.; Komaromi, I.; Gomperts, R.; Martin, R. L.; Fox, D. J.; Keith, T.; Al-Laham, M. A.; Peng, C. Y.; Nanayakkara, A.; Gonzalez, C.; Challacombe, M.; Gill, P. M. W.; Johnson, B. G.; Chen, W.; Wong, M. W.; Andres, J. L.; Head-Gordon, M.; Replogle, E. S.; Pople, J. A. *Gaussian 98*, revision A.7; Gaussian, Inc.: Pittsburgh, PA, 1998.

(23) (a) Bickelhaupt, F. M.; Baerends, E. J. *Rev. Comput. Chem.* **2000**, 15, 1. (b) te Velde, G.; Bickelhaupt, F. M.; Baerends, E. J.; van Gisbergen, S. J. A.; Fonseca Guerra, C.; Snijders, J. G.; Ziegler, T. *J. Comput. Chem.* **2001**, 22, 931.

(24) Hay, P. J.; Wadt, W. R. *J. Phys. Chem.* **1985**, 82, 299.

(25) Frenking, G.; Antes, I.; Böhme, M.; Dapprich, S.; Ehlers, A. W.; Jonas, V.; Neuhaus, A.; Otto, M.; Stegmann, R.; Veldkamp, A.; Vyboishchikov, S. F. In *Reviews in Computational Chemistry*; Lipkowitz, K. B., Boyd, D. B., Eds.; VCH: New York, 1996; Vol. 8, p 63–144.

(26) Snijders, J. G.; Baerends, E. J.; Vernooijs, P. *At. Data Nucl. Data Tables* **1982**, 26, 483.

(27) (a) Snijders, J. G. *Mol. Phys.* **1978**, 36, 1789. (b) Snijders, J. G.; Ros, P. *Mol. Phys.* **1979**, 38, 1909.

(28) Baerends, E. J.; Ellis, D. E.; Ros, P. *Chem. Phys.* **1973**, 2, 41.

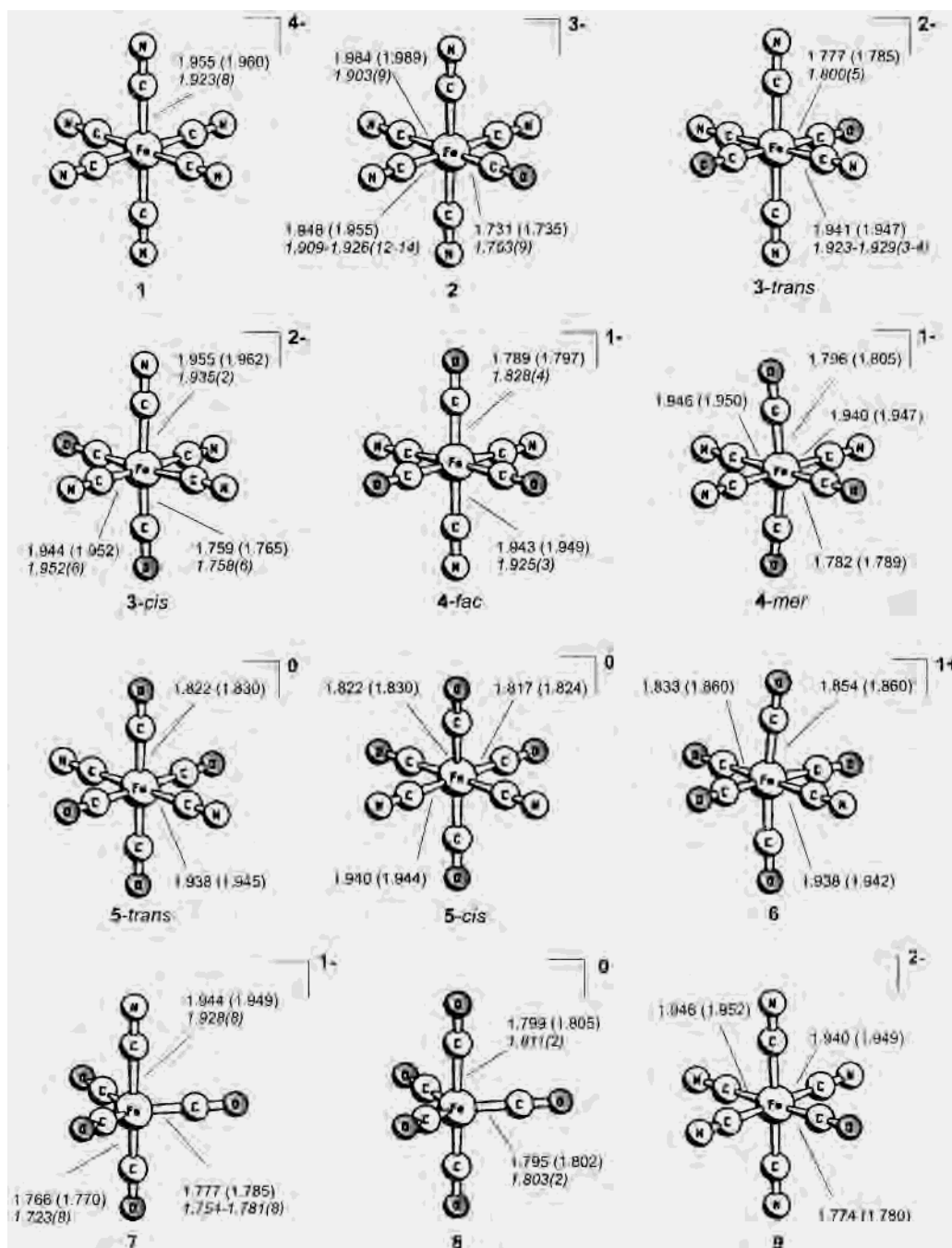


Figure 1. Calculated structures $[\text{Fe}(\text{CO})_4(\text{CN})_2]_q$ and metal–ligand bond distances at BP86/II [Å]. BP86/TZP values are given in parentheses. Experimental bond lengths are given in italics, taken from refs 3, 4, 6, 8, 9a, and 9c.

bonding, the ratio of $\Delta E_{\text{elsta}}/\Delta E_{\text{orb}}$ indicates the electrostatic and covalent nature of the bond. Furthermore, the contributions of σ and π bonding to a covalent multiple bond can be determined by partitioning the ΔE_{orb} term into the contributions by orbitals that belong to different irreducible representations of the point group of the interacting system.

The bond dissociation energy $D_e = -\Delta E_e$ can be determined from ΔE_{int} and the fragment preparation energy ΔE_{prep} , which is the energy necessary to promote fragments from their equilibrium geometry and electronic ground state to the geometry and electronic state of the optimized structure:

$$\Delta E_e = \Delta E_{\text{prep}} + \Delta E_{\text{int}} \quad (2)$$

Further details about the method can be found in the literature.^{23a}

Results and Discussion

Geometries and Vibrational Spectra. Figure 1 shows the optimized structures of the complexes 1–9 and the calculated values of the Fe–CO and Fe–CN bond lengths at BP86/II (BP86/TZP). Tables with complete sets of coordinates are given as Supporting Information. Experimental bond lengths which were determined by X-ray structure analysis are shown in italics.

The calculated Fe–CO and Fe–CN distances at BP86 using the larger basis set TZP are always slightly longer (0.005–0.010 Å) than the BP86/II values, but the differences are not very large and need not be further discussed. The experimental iron–ligand bond lengths of the all-cyano

Table 1. Comparison of the Experimental and Theoretical C–O and C–N Stretching Modes at BP86/II^f

compd	BP86/II							experiment			
	$\nu(\text{CO})$	$\nu(\text{CN})$	IR int	Raman act.	ir rep	$\nu(\text{CO})$	$\nu(\text{CN})$	IR int	Raman act.		
1	[D _{6h}]	[Fe(CN) ₆] ⁴⁻		1998	540	0.0	T _{2u}				
2	[C _{4v}]	[FeCO(CN) ₅] ³⁻	1890		829	18	A ₁	1931 ^b	2044 ^a	strong	
				2108	17	258	A ₁			strong	
				2094	52	166	A ₁		2095	shoulder	
				2083	0.0	219	B ₂				
				2073	275	0.4	E		2075	strong	
3-trans	[D _{4h}]	trans-[Fe(CO) ₂ (CN) ₄]	2021		0.0	87	A _{1g}	2067			medium ^g
			1960		1463	0.0	A _{2u}	1992 ^c		medium	
				2143	0.0	265	A _{1g}		2121		
				2128	0.0	188	B _{1g}		2112		medium
				2119	147	0.0	E _u		2104		medium
3-cis	[C _{2v}]	cis-[Fe(CO) ₂ (CN) ₄] ²⁻	1995		612	21	A ₁	2022 ^d		strong	
			1953		844	37	B ₂	1967		strong	
				2148	6.4	200	A ₁				
				2139	35	95	B ₂		2106	medium	
				2135	16	155	A ₁				
				2123	127	0.0	B ₁		2080	medium	
4-fac	[C _{3v}]	fac-[Fe(CO) ₃ (CN) ₃] ¹⁻	2075		440	31	A ₁	2121 ^d		medium	weak
			2025		678	59	E	2096		strong	medium
				2174	0.01	161	A ₁		2162	weak	medium
				2167	9	83	E		2140	weak	medium
4-mer	[C _{2v}]	mer-[Fe(CO) ₃ (CN) ₃] ¹⁻	2094		24	88	A ₁				
			2036		1101	5.5	B ₂				
			2028		616	63	A ₁				
				2155	48	0.3	B ₁				
				2164	6.0	116	A ₁				
				2172	0.0	197	A ₁				
5-trans	[D _{4h}]	trans-[Fe(CO) ₄ (CN) ₂]	2154 ^e		0.0	106	A _{1g}				
			2114		0.0	153	B _{1g}				
			2089		857	0.0	E _u				
				2189	0.0	186	A _{1g}				
				2176	5.7	0.0	A _{2g}				
5-cis	[C _{2v}]	cis-[Fe(CO) ₄ (CN) ₂]	2146		49	81	A ₁				
			2096		789	7	B ₁				
			2095		404	88	A ₁				
			2079		518	76	B ₂				
				2186	7.9	143	A ₁				
				2181	0.2	76	B ₂				
6	[C _{4v}]	[Fe(CO) ₅ CN] ¹⁺	2197 ^e		32	159	A ₁				
			2139		567	1.5	E				
			2133		330	96	A ₁				
				2184	3.5	58	A ₁				
				2157	0.0	154	B ₂				
7	[C _{3v}]	[Fe(CO) ₄ CN] ¹⁻	2023		136	17	A ₁	2040 ^f		not reported	
			1951		652	54	A ₁	1951		not reported	
			1948		1137	42	E	1933		not reported	
				2140	27	124	A ₁		2118	not reported	
8	[D _{3h}]	[Fe(CO) ₅]	2109		0.0	55	A ₁ '	2121 ^h			not reported
			2037		0.0	121	A ₁ '	2042			not reported
			2031		1148	0	A ₂ ''	2034		strong	
			2018		966	51	E'	2013		strong	not reported
9	[C _{4v}]	[Fe(III)CO(CN) ₅] ²⁻	1997		644	42	A ₁	2064 ^b		strong	
				2153	14	144	A ₁		2098	not reported	
				2125	3	802	A ₁				
				2116	0.0	727	B ₂				
				2111	0.2	0.2	E				

^a Reference 6. ^b Reference 8. ^c Reference 3. ^d Reference 4. ^e This mode is a simultaneous CO/CN-mode. ^f Reference 9a. ^g Raman data are taken from a personal communication with Koch. ^h Reference 9b. ⁱ Frequencies in cm⁻¹, IR intensities in KM mol⁻¹, Raman activities in Å⁴ amu⁻¹.

complex [Fe(CN)₆]⁴⁻ (**1**) and the all-carbonyl complex [Fe(CO)₅] (**8**) which may be used as reference values indicate that the theoretical Fe–CN distances are slightly longer than the values which are obtained through X-ray structure analysis while the calculated Fe–CO bonds are a bit shorter than the experimental data, but the differences are not very large. We want to point out that the BP86 calculations predict that the axial Fe–CO bond in iron pentacarbonyl is longer than the equatorial bond which is in agreement with experiment. In a previous theoretical study we found that

the bond lengths of donor–acceptor bonds tend to become shorter in the solid state because of interatomic interactions.²⁹ Deeth et al. reported a similar effect for transition metal complexes with carbonyl and chloride ligands.³⁰

A comparison of the calculated and experimental metal–ligand bond lengths of [Fe(CN)₅CO]³⁻ (**2**) shows some

(29) Jonas, V.; Frenking, G.; Reetz, M. T. *J. Am. Chem. Soc.* **1994**, *116*, 8741.

(30) Bray, M. R.; Deeth, R. J.; Paget, V. J.; Sheen, P. D. *Int. J. Quantum Chem.* **1996**, *61*, 85.

Table 2. ETS Analysis of the Fe–CO bond with CN[−] in Trans Position at BP86/TZP^c

	2	3-cis	4-fac	4-mer	5-cis	6	7	9
$r(\text{[Fe]}-\text{L})$	1.74	1.77	1.80	1.79	1.82	1.86	1.77	1.78
[Fe]	Fe(CN) ₅ ^{3−}	Fe(CO)(CN) ₄ ^{2−}	Fe(CO) ₂ (CN) ₃ [−]	Fe(CO) ₂ (CN) ₃ [−]	Fe(CO) ₃ (CN) ₂	FeCN(CO) ₄ ¹⁺	FeCN(CO) ₃ ^{1−}	Fe(CN) ₅ ^{2−}
L	CO	CO	CO	CO	CO	CO	CO	CO
ΔE_{int}	−62.7	−49.1	−42.0	−45.0	−42.4	−45.9	−63.1	−45.2
ΔE_{Pauli}	181.9	172.4	161.3	156.7	140.9	114.6	147.5	165.0
ΔE_{elstat}	−127.1(51.9%) ^a	−120.0(54.2%)	−112.3(55.2%)	−110.6(54.8%)	−100.7(54.9%)	−86.0(53.6%)	−108.0(51.3%)	−115.4(54.9%)
ΔE_{orb}	−117.6(48.1%) ^a	−101.4(45.8%)	−91.0(44.8%)	−91.2(45.2%)	−82.6(45.1%)	−74.5(46.4%)	−102.6(48.7%)	−94.8(45.1%)
ΔE_{σ}	−46.5(39.6%) ^b	−45.5(44.9%)	−49.4(54.3%)	−47.6(52.2%)	−48.2(58.4%)	−45.5(61.1%)	−42.7(41.6%)	−46.0(48.6%)
ΔE_{π}	−70.3(59.8%) ^b	−55.9(55.1%)	−41.6(45.7%)	−43.3(47.5%)	−34.4(41.6%)	28.9(38.8%)	−59.9(58.3%)	−47.3(49.9%)
ΔE_{prep}	10.8	7.0	4.9	5.3	3.5	1.7	3.7	8.0
ΔE	−51.9	−42.1	−37.2	−39.7	−38.9	−44.3	−59.4	−37.2
(=−D _c)								

^a Contribution to the whole attractive interaction $\Delta E_{\text{elstat}} + \Delta E_{\text{orb}}$. ^b Contribution to the whole orbital interaction ΔE_{orb} . ^c Energies in kcal/mol, bond length in Å.

Table 3. ETS Analysis of the Fe–CO Bond with CO in Trans Position at BP86/TZP^c

	3-trans	4-mer	5-trans	5-cis	6	7	8
$r(\text{[Fe]}-\text{L})$	1.79	1.81	1.83	1.83	1.86	1.79	1.80
[Fe]	Fe(CO)(CN) ₄ ^{2−}	Fe(CO) ₂ (CN) ₃ [−]	Fe(CO) ₃ (CN) ₂	Fe(CO) ₃ (CN) ₂	FeCN(CO) ₄ ¹⁺	FeCN(CO) ₃ ^{1−}	Fe(CO) ₄
L	CO	CO	CO	CO	CO	CO	CO
ΔE_{int}	−43.2	−40.5	−41.0	−40.6	−44.5	−53.2	−54.6
ΔE_{Pauli}	159.2	155.5	144.5	149.8	131.6	164.1	134.8
ΔE_{elstat}	−110.8(54.8%) ^a	−107.8(55.0%)	−100.4(54.1%)	−103.5(54.4%)	−92.5(52.5%)	−119.1(54.8%)	−98.0(51.7%)
ΔE_{orb}	−91.6(45.2%) ^a	−88.1(45.0%)	−85.1(45.9%)	−86.9(45.7%)	−83.7(47.5%)	−98.3(45.2%)	−91.4(48.3%)
ΔE_{σ}	−46.1(50.3%) ^b	−50.2(56.9%)	−54.0(63.5%)	−55.7(64.1%)	−57.4(68.6%)	−29.1(29.7%)	−47.6(52.1%)
ΔE_{π}	−45.0(49.1%) ^b	−38.0(43.1%)	−30.9(36.3%)	−31.2(35.9%)	−26.2(31.4%)	−69.1(70.3%)	−43.8(47.9%)
ΔE_{prep}	7.3	5.5	5.0	4.3	3.7	8.6	8.1
ΔE	−35.9	−35.0	−35.9	−36.3	−40.9	−44.6	−46.5
(=−D _c)							

^a Contribution to the whole attractive interaction $\Delta E_{\text{elstat}} + \Delta E_{\text{orb}}$. ^b Contribution to the whole orbital interaction ΔE_{orb} . ^c Energies in kcal/mol, bond length in Å.

differences between theory and experiment. The theoretically predicted Fe–CO distance (1.731 and 1.735 Å) is slightly shorter than the experimental value (1.753 Å) like in iron pentacarbonyl while the Fe–CN distance which is trans to Fe–CO is significantly longer (1.984 and 1.989 Å) than the observed value (1.903 Å). Another surprising result is that the calculations predict the Fe–CN distance which is trans to Fe–CO to be clearly longer than the Fe–CN bond length that is trans to another Fe–CN bond (1.948 and 1.955 Å) while the X-ray structure analysis give the opposite trend (Figure 1). The experimentally derived data indicate that the Fe–CN_{trans} distance is slightly shorter than the Fe–CN_{cis} bond length (1.915 Å). A similar discrepancy between theory and experiment is found for the complexes **3-cis** and **4-mer**. The calculations predict that the Fe–CN bonds which are trans to CO are slightly longer than the Fe–CN bonds which are trans to another CN[−] ligand while the X-ray structure analysis gives the opposite trend. It is possible that intermolecular forces between the highly charged species yield significant changes of the bond lengths of the free molecules. The calculated metal–carbon bond lengths of the remaining complexes **3-trans**, **4-fac**, and **7** are in reasonable agreement with the experimental values (Figure 1). Note, however, that the calculated Fe–CO bond length of **4-fac** (1.789 and 1.797 Å) is somewhat shorter than the experimental value (1.828 Å). According to the calculations, the oxidation of the Fe(II) complex [Fe(CN)₅CO]^{3−} (**2**) to the Fe(III) species [Fe(CN)₅CO]^{2−} (**9**) yields a significant lengthening of the Fe–CO bond and a clearly shorter Fe–CN_{trans} bond while the Fe–CN_{cis} bond length remains nearly the same.

Table 1 gives the calculated and experimental vibrational frequencies and the Raman activities and IR intensities. The C–O stretching frequencies lie between 20 cm^{−1} (compound **3**) and 70 cm^{−1} (compound **4-fac**) below the experimental values. Thiel et al. have reported a similar effect during the investigation of pure transition metal–carbonyl complexes with the BP86 functional. They proposed a shift factor of 28.3 cm^{−1} for the prediction of frequencies for this class of compounds.¹⁸ Interestingly, the theoretical C–N frequencies lie in most cases above the experimental values. The different performance of the BP86/II calculated frequencies becomes obvious when Figure 2 is considered which shows a plot of the theoretical and experimental vibrational frequencies of the C–O and C–N stretching modes.

The calculated vibrational modes suggest that the C–O stretching frequency of the octahedral Fe(II) complexes [Fe(CN)_n(CO)_{6−n}]^q is shifted toward higher wavenumbers when *n* becomes smaller which is in agreement with experiment (Table 1). The same trend is predicted for the C–N stretching mode, but the increase is not as steep as for the C–O fundamental. The theoretically predicted frequencies and intensities listed in Table 1 should be a helpful guideline for the identification of the yet unknown species of the series. A pertinent example is the Fe(III) complex [Fe(CN)₅CO]^{2−} (**9**) which could not be identified by X-ray structure analysis. After oxidation of the Fe(II) complex [Fe(CN)₅CO]^{3−} (**2**), Koch et al. could only detect a species with an IR frequency of 2064 cm^{−1} (compound **2**: 1931 cm^{−1}).⁹ We calculated a shift of more than 100 cm^{−1} upon oxidation of compound **2** to compound **9** which supports the hypothesis that the latter

Table 4. ETS Analysis of the Fe–CN Bond with CO in Trans Position at BP86/TZP^c

	2	3-cis	4-fac	4-mer	5-cis	6	7	9
$r([\text{Fe}]-\text{L})$	1.99	1.96	1.95	1.95	1.94	1.94	1.95	1.95
[Fe]	$\text{FeCO}(\text{CN})_4^{2-}$	$\text{Fe}(\text{CO})_2(\text{CN})_3^{1-}$	$\text{Fe}(\text{CO})_3(\text{CN})_2$	$\text{Fe}(\text{CO})_3(\text{CN})_2$	$\text{Fe}(\text{CO})_4(\text{CN})^+$	$\text{Fe}(\text{CO})_5^{2+}$	$\text{Fe}(\text{CO})_4$	$\text{Fe}(\text{CO})(\text{CN})_4^{1-}$
L	CN^-	CN^-	CN^-	CN^-	CN^-	CN^-	CN^-	CN^-
ΔE_{int}	81.7	-7.3	-100.1	-104.0	-202.3	-312.2	-94.3	-13.2
ΔE_{Pauli}	125.8	146.0	163.0	162.1	171.0	162.6	144.0	144.9
ΔE_{elstat}	26.3	-67.6(44.1%) ^a	-160.7(61.1%)	-162.9(61.2%)	-254.3(68.1%)	-343.3(72.3%)	-147.7(62.0%)	-69.8(44.2%)
ΔE_{orb}	-70.4	-85.6(55.8%) ^a	-102.4(38.9%)	-103.1(38.8%)	-119.0(31.9%)	-131.5(27.7%)	-90.7(38.0%)	-88.3(55.8)
ΔE_{σ}	-56.2(79.8%) ^b	-70.5(82.4%)	-84.7(82.6%)	-85.9(83.3%)	-94.5(79.5%)	-100.4(76.4%)	-70.8(78.1%)	-71.0(80.4%)
ΔE_{π}	-12.6(17.8%) ^b	-15.1(17.7%)	-17.8(17.4%)	-16.4(15.9%)	-24.4(20.5%)	-28.8(21.9%)	-19.7(21.7%)	-12.7(14.6%)
ΔE_{prep}	4.6	3.7	3.0	4.9	3.8	3.6	2.0	5.2
ΔE	-86.3	-3.6	-97.1	-99.1	-198.4	-308.6	-92.3	-8.0

(=-D_e)

^a Contribution to the whole attractive interaction $\Delta E_{\text{elstat}} + \Delta E_{\text{orb}}$. ^b Contribution to the whole orbital interaction ΔE_{orb} . ^c Energies in kcal/mol, bond length in Å.

Table 5. ETS Analysis of the Fe–CN Bond with CN in Trans Position at BP86/TZP^c

	1	2	3-trans	3-cis	4-mer	5-trans
$r([\text{Fe}]-\text{L})$	1.96	1.96	1.95	1.95	1.95	1.95
[Fe]	$\text{Fe}(\text{CN})_5^{3-}$	$\text{FeCO}(\text{CN})_4^{2-}$	$\text{Fe}(\text{CO})_2(\text{CN})_3^{1-}$	$\text{Fe}(\text{CO})_2(\text{CN})_3^{1-}$	$\text{Fe}(\text{CO})_3(\text{CN})_2$	$\text{Fe}(\text{CO})_4(\text{CN})^+$
L	CN^-	CN^-	CN^-	CN^-	CN^-	CN^-
ΔE_{int}	155.9	74.7	-13.7	-11.1	-104.6	-203.7
ΔE_{Pauli}	131.0	142.8	149.3	154.4	156.7	152.5
ΔE_{elstat}	96.3	9.5	-78.1(47.9%) ^a	-78.3(47.3%)	-166.0(63.5%)	-252.2(70.8%)
ΔE_{orb}	-71.4	-77.6	-84.9(52.1%) ^a	-87.1(52.6%)	-95.4(36.5%)	-104.0(29.2%)
ΔE_{σ}	-52.1(72.9%) ^b	-60.8(78.3%)	-70.1(82.6%)	-71.5(82.0%)	-78.5(82.3%)	-83.9(80.7%)
ΔE_{π}	-18.0(25.2%) ^b	-16.9(21.7%)	-14.1(16.6%)	-15.7(18.0%)	-16.9(17.7%)	-18.6(17.8%)
ΔE_{prep}	6.6	4.8	5.2	3.6	3.3	2.6
ΔE	162.5	79.5	-8.5	-7.5	-101.3	-201.1

(=-D_e)

^a Contribution to the whole attractive interaction $\Delta E_{\text{elstat}} + \Delta E_{\text{orb}}$. ^b Contribution to the whole orbital interaction ΔE_{orb} . ^c Energies in kcal/mol, bond length in Å.

species was indeed prepared by Koch. According to the theoretical Raman frequencies, complex **9** should also be distinguishable from the reduced species by its very strong Raman signal at $\sim 2120 \text{ cm}^{-1}$.

Bonding Analysis. The results of the EPA of the Fe–CO and Fe–CN⁻ bonds are shown in Tables 2–5. The bonding analyses were carried out using one ligand CO or CN⁻ and the remaining metal fragment in the low-spin state where the metal has a closed-shell t_{2g}^6 -like configuration as interacting species. The presentation of the results follows an ordering scheme where we first give the data of the Fe–CO bonds which are trans to a cyano ligand (Table 2). Next we show the results of the Fe–CO bonds which are trans to another carbonyl ligand (Table 3). Table 4 gives the EPA results for the Fe–CN⁻ bonds which are trans to CO while Table 5 shows the results for Fe–CN⁻ bonds trans to CO.

The carbonyl ligand is usually considered as a strong π acceptor. A previous EPA study of the isoelectronic complexes $[\text{TM}(\text{CO})_6]^q$ (TM^q = Hf²⁺, Ta⁻, W, Re⁺, Os²⁺, Ir³⁺) has shown that the metal–ligand π -orbital interactions between one CO ligand and the $[\text{TM}(\text{CO})_5]^q$ fragment contribute between 56.6% ($[\text{Hf}(\text{CO})_6]^{2-}$) and 26.2% ($[\text{Ir}(\text{CO})_6]^{3+}$) to the total ΔE_{orb} term. An increase of the π -orbital interactions when the complexes become more negatively charged is also found for the mixed carbonyl/cyano complexes which are studied here. Tables 2 and 3 show that, in the hexacoordinated Fe(II) complexes **2–6**, the calculated values of the absolute and relative contributions of ΔE_{π} to the bonding interactions increases from the positively charged species **6** to the trianion **2**. Note that the

total contribution of the orbital term to the attractive interactions remains rather constant between 45% and 48%. The EDA results show that the Fe–CO binding interactions which are trans to CN⁻ (Table 2) have a significantly larger π -contribution than the Fe–CO bonds in the same complex which are trans to CO (see complexes **4-mer**, **5-cis**, **6**, Table 3). Note, however, that the axial Fe–CO bond of the pentacoordinated complex **7** has less π -contribution than the equatorial Fe–CO bonds which do not have a ligand that is trans to the carbonyl group. We also want to point out that the oxidation of the Fe(II) complex **2** to the Fe(III) complex **9** weakens the iron–carbonyl π -interactions which is the reason that the orbital contributions in the latter compound and, thus, the strength of the Fe–CO bond is reduced (Table 2).

It is generally said that the strength of the metal–CO π -interactions has a strong influence on the C–O stretching frequency which is therefore often used as a probe of the π -bonding. A charge partitioning analysis of $(\text{CO})_5\text{W}-\text{L}$ complexes with various ligands L using the CDA method³² showed that there is indeed a correlation between the amount of $\text{W} \rightarrow \text{L}$ π -back-donation and the calculated vibrational mode of the carbonyl ligand.^{13a} Figure 3 shows a plot of the theoretically predicted C–O stretching frequencies and the energy contribution of ΔE_{π} to the bonding interactions. There is a good correlation between ΔE_{π} and $\nu(\text{CO})$ which changes toward higher wavenumbers when ΔE_{π} becomes less.

(31) Diefenbach, A.; Bickelhaupt, F. M.; Frenking, G. *J. Am. Chem. Soc.* **2000**, *122*, 6449.

(32) Dapprich, S.; Frenking, G. *J. Phys. Chem.* **1995**, *99*, 9352.

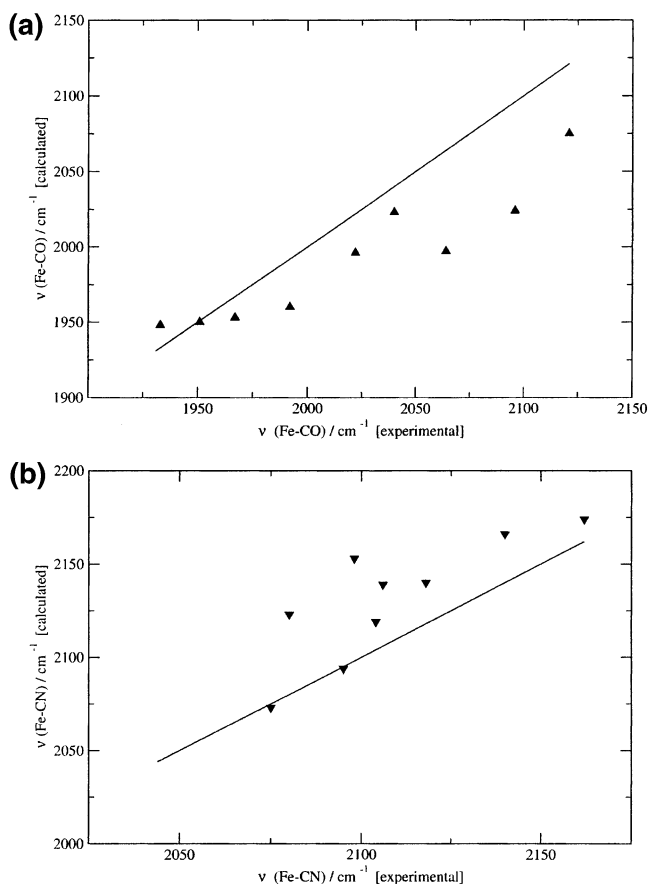


Figure 2. (a) Calculated vs. experimental C–O stretching modes (and straight line with slope 1). (b) Calculated vs. experimental C–N stretching modes (and straight line with slope 1).

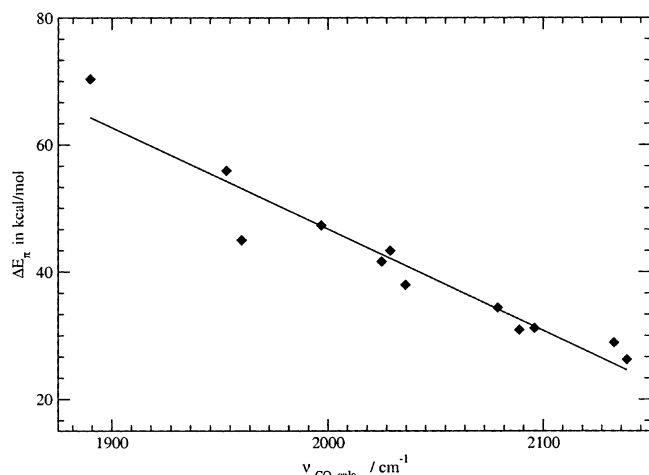


Figure 3. Correlation of calculated C–O stretching modes and ΔE_{π} (and regression line).

Tables 4 and 5 give the EPA results of the iron–cyano bonds. Note that some complexes are thermodynamically unstable with regard to dissociation of CN^- because of strong Coulomb repulsion between the ligand and the negatively charged metal fragment. We want to point out that the absolute values of the interaction energies and the energy terms of complexes which carry different charges should not be compared with each other because the charges have a strong influence on the calculated values particularly for ΔE_{int} and ΔE_{elstat} . The EPA results are nevertheless meaningful

because they give insight into the relative strength of the σ - and π -interactions.

The cyano ligand CN^- is generally considered as a strong σ -donor and a poor π -acceptor unlike the good π -acceptor CO because the negatively charged CN^- has a high-lying unoccupied π^* MO. The EPA results in Tables 4 and 5 show that the π -contribution to the iron–cyano orbital interactions is indeed much smaller compared to the iron–carbonyl bonding (Tables 2 and 3). There is no correlation between the charge of the complexes and the strength of ΔE_{π} of the Fe– CN^- complexes such as in case of the Fe–CO bond. Note that the largest value for ΔE_{π} in the hexacoordinated complexes is found for the interactions between $\text{Fe}(\text{CO})_5^{2+}$ and CN^- in the positively charged species **6** (Table 4). It is highly unlikely that the comparatively large ΔE_{π} value comes from $\text{Fe} \rightarrow \text{CN}^-$ π -back-donation. Rather, it may partly arise from $\text{Fe} \leftarrow \text{CN}^-$ π -donation which has previously been suggested to play a role in metal–CO bonding.³³ The Fe– CN^- bonds which are trans to CO have weaker contributions from π -back-donation than Fe– CN^- bonds in the same complex which are trans to CN^- , but the differences are not very large. The $\text{Fe} \rightarrow \text{L}$ π -back-donation plays a much bigger role for the stretching frequencies of $\text{L} = \text{CO}$ than for $\text{L} = \text{CN}^-$. Note that the highest lying C–O stretching frequency increases from **2** (1890 cm^{-1}) to **6** (2197 cm^{-1}) by 307 cm^{-1} while the C–N stretching mode increase from **2** (2108 cm^{-1}) to **6** (2184 cm^{-1}) by only 76 cm^{-1} .

Summary and Conclusion

The calculated geometries and vibrational frequencies of the iron cyano/carbonyl complexes **1–9** are in good agreement with most experimental data. The theoretical data will be useful for the identification of the yet unknown members of the series $[\text{Fe}(\text{CN})_x(\text{CO})_y]^q$. The energy partitioning analysis of the Fe–CO bonds shows that the binding interactions in all complexes have $\sim 55\%$ electrostatic character and only $\sim 45\%$ covalent character. There is a significant contribution of the π -orbital interaction to the Fe–CO covalent bonding which increases when the complexes become negatively charged. The strength of ΔE_{π} may even be larger than ΔE_{σ} . The calculated binding energy of the Fe–CO π -interactions correlates very well with the C–O stretching frequencies. The Fe– CN^- bonds have much less π -character than the Fe–CO bonds.

Acknowledgment. This work was supported by the Deutsche Forschungsgemeinschaft and by the Fonds der Chemischen Industrie. We wish to thank Professor Stephen Koch for information about unpublished work. Excellent service by the Hochschulrechenzentrum of the Philipps-Universität Marburg is gratefully acknowledged.

Supporting Information Available: Cartesian coordinates and energies. This material is available free of charge via the Internet at <http://pubs.acs.org>.

IC034807E

(33) Ref 12a, page 227.